Electronic Supplementary Material (ESI) for Journal of Materials Chemistry A.

Supplementary Information

Guidelines for designing high-deformability materials for all-solid-state lithium-ion batteries

Naoto Tanibata,[*a] *Shin Aizu,*[a] *Misato Koga,*[a] *Hayami Takeda,*[a] *Ryo Kobayashi*[b] *and Masanobu Nakayama*[a]

[a.] *Department of Advanced Ceramics, Nagoya Institute of Technology, Gokiso, Showa, Nagoya, Aichi 466-8555, Japan.*

[b.] *Department of Applied Physics, Nagoya Institute of Technology, Gokiso, Showa, Nagoya, Aichi 466-8555, Japan.*

* Corresponding Author. E-mail: tanibata.naoto@nitech.ac.jp

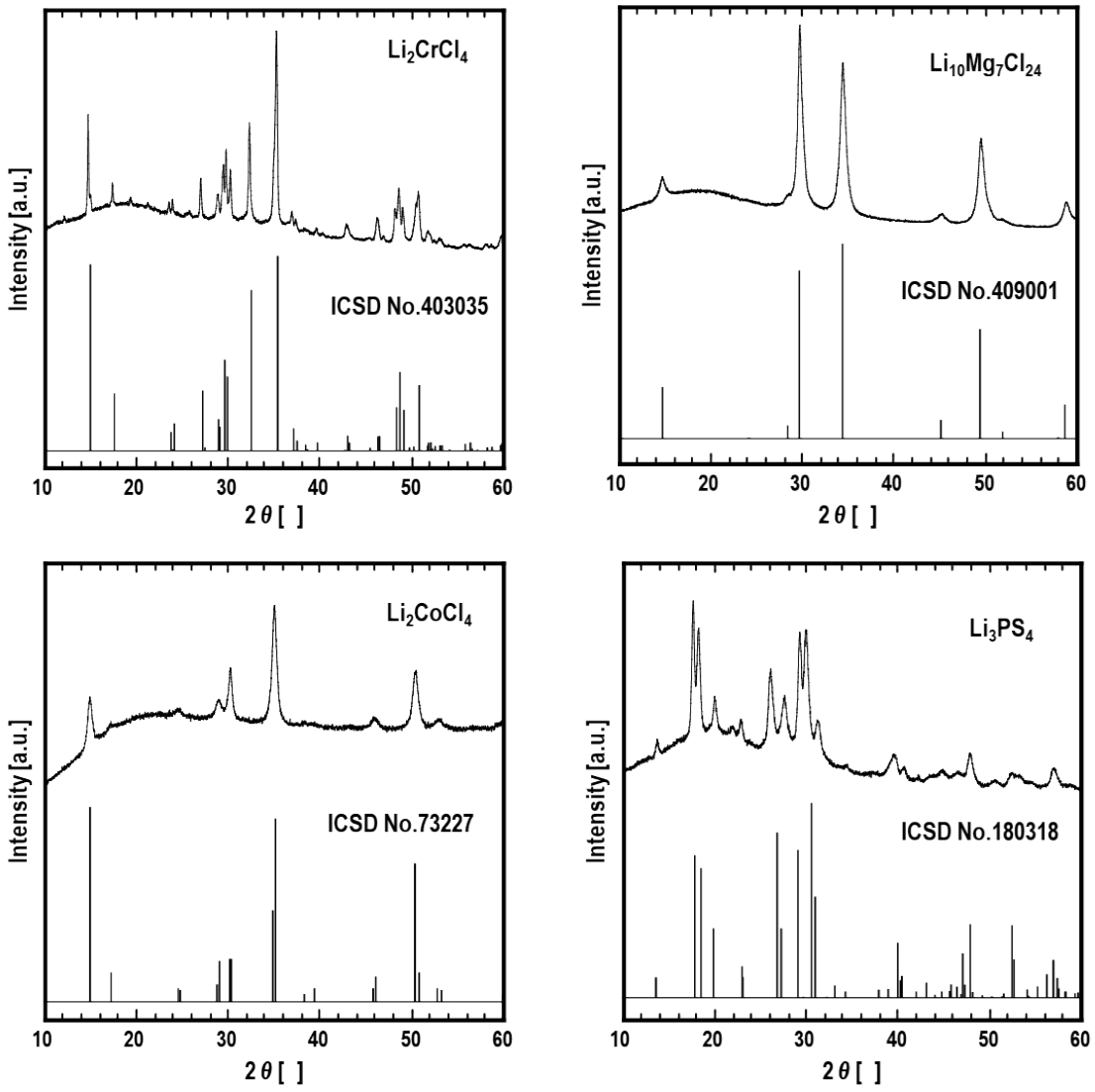

Fig. S1. XRD patterns of the four materials synthesised in this study (Li_2CrCl_4, $Li_{10}Mg_7Cl_{24}$, Li_2CoCl_4, and Li_3PS_4). The peaks for all four materials are consistent with those listed in the inorganic crystal structure database (ICSD), confirming that the target materials were successfully synthesised.

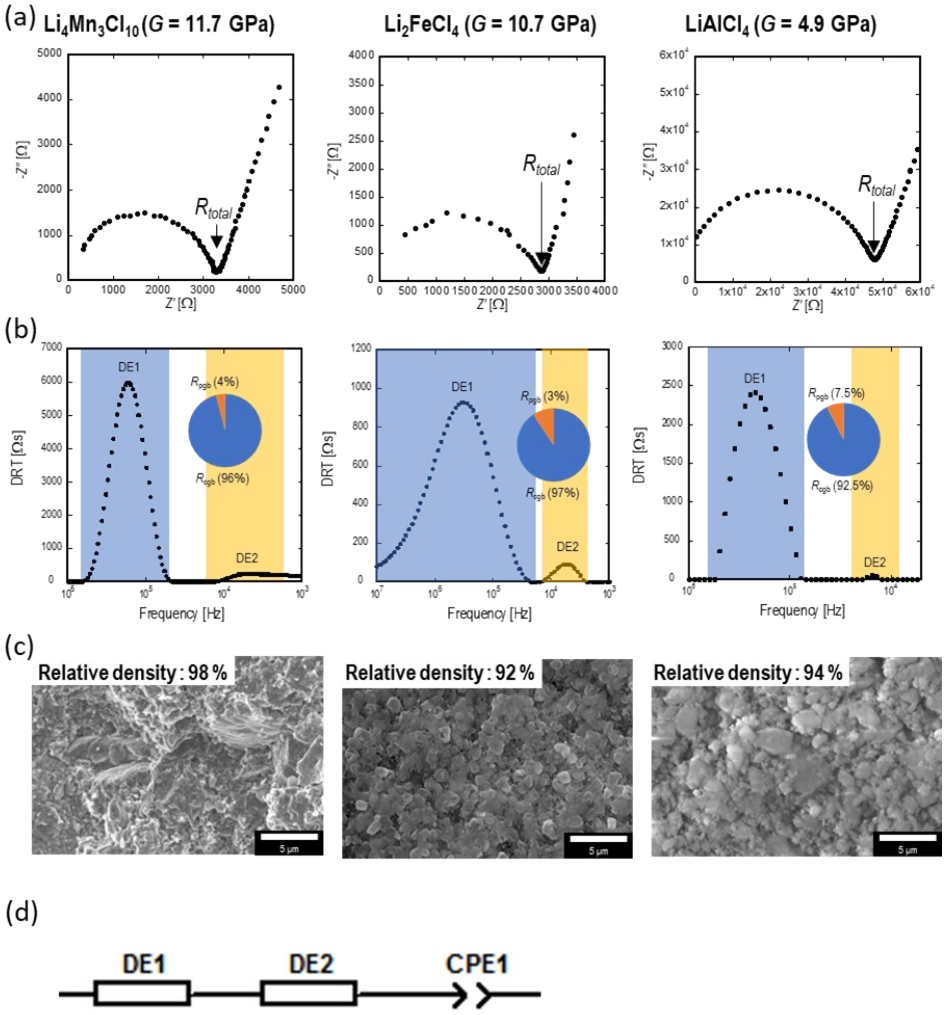

Fig. S2. Characterisation of pellets of the chlorides $Li_4Mn_3Cl_{10}$, Li_2FeCl_4, and $LiAlCl_4$. (a) AC impedance results (Nyquist plots). (b) DRT spectra. The pie chart shows the relative magnitudes of the crystallite grain boundary resistance R_{cgb} and particle grain boundary resistance R_{pgb}. (c) Cross-sectional SEM images of the pellets; the relative densities are indicated. (d) Equivalent circuit used for fitting.

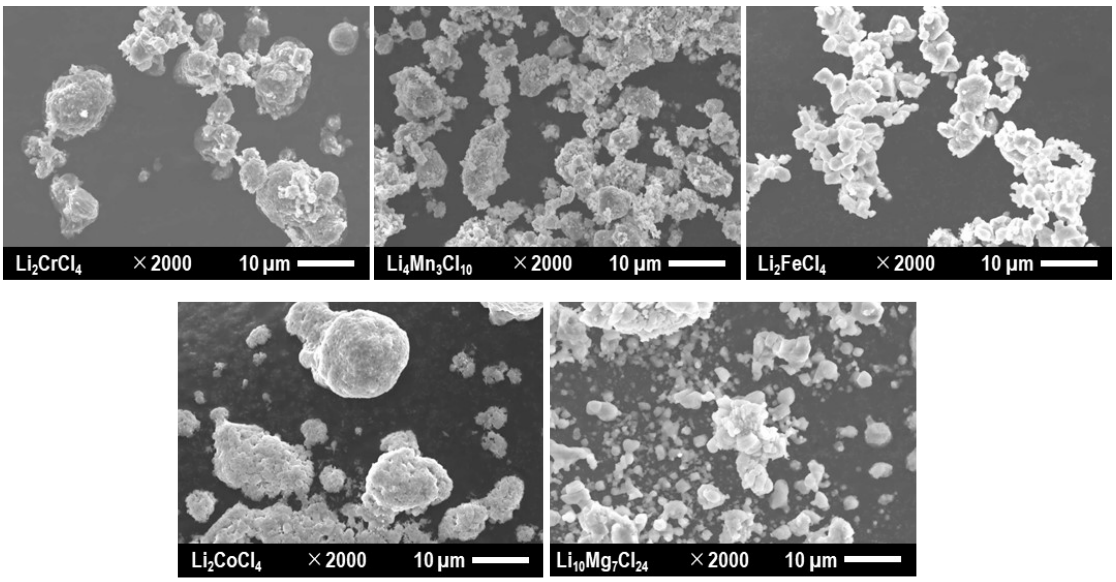

Fig. S3. Cross-sectional SEM images of Li_2CrCl_4, $Li_4Mn_3Cl_{10}$, Li_2FeCl_4, Li_2CoCl_4, and $Li_{10}Mg_7Cl_{24}$ powders.

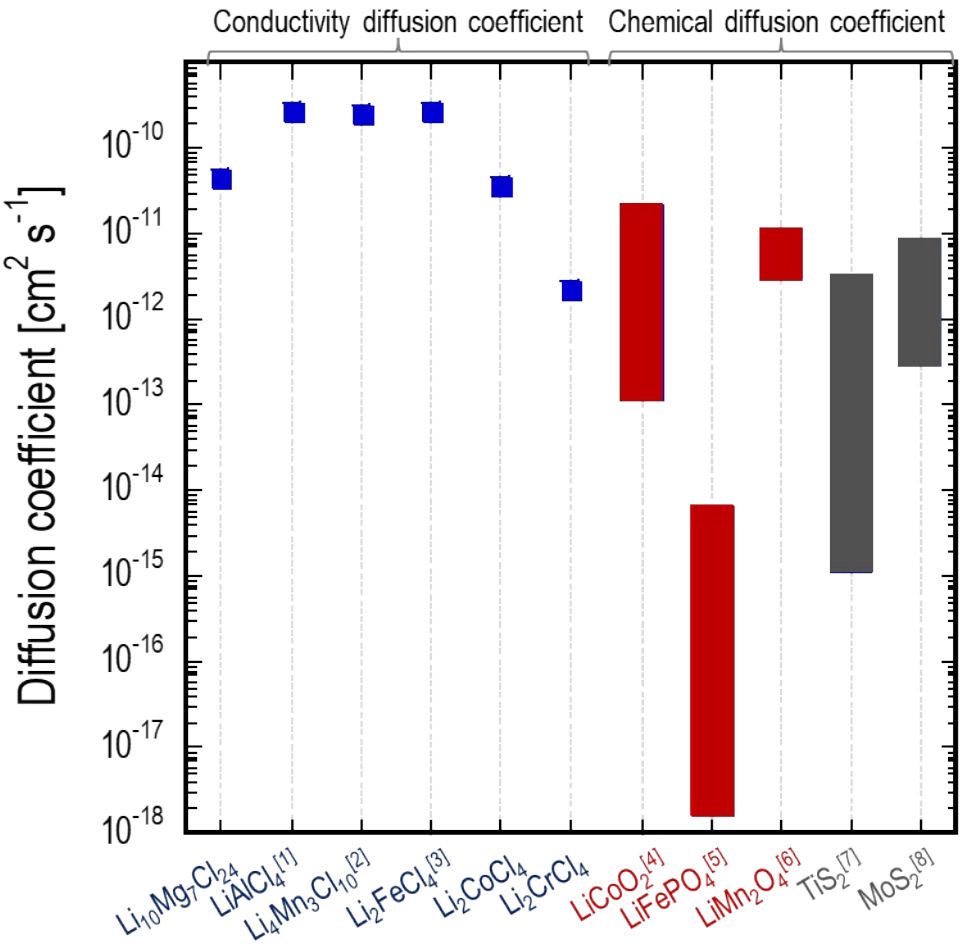

Fig. S4. Diffusion coefficients of the chloride materials ($Li_{10}Mg_7Cl_{24}$, $LiAlCl_4$,[1] $Li_4Mn_3Cl_{10}$,[2] Li_2FeCl_4,[3] Li_2CoCl_4, and Li_2CrCl_4) computationally screened in this study, and typical oxide ($LiCoO_2$,[4] $LiFePO_4$,[5] and $LiMn_2O_4$[6]) and sulfide (TiS_2[7] and MoS_2[8]) cathode materials. The chloride materials generally exhibit higher Li diffusivity than the typical oxide and sulfide cathode materials. Moreover, the chloride materials exhibit even larger Li chemical diffusion coefficients because those calculated from ionic conductivity assuming a thermodynamic factor of unity are often underestimated.

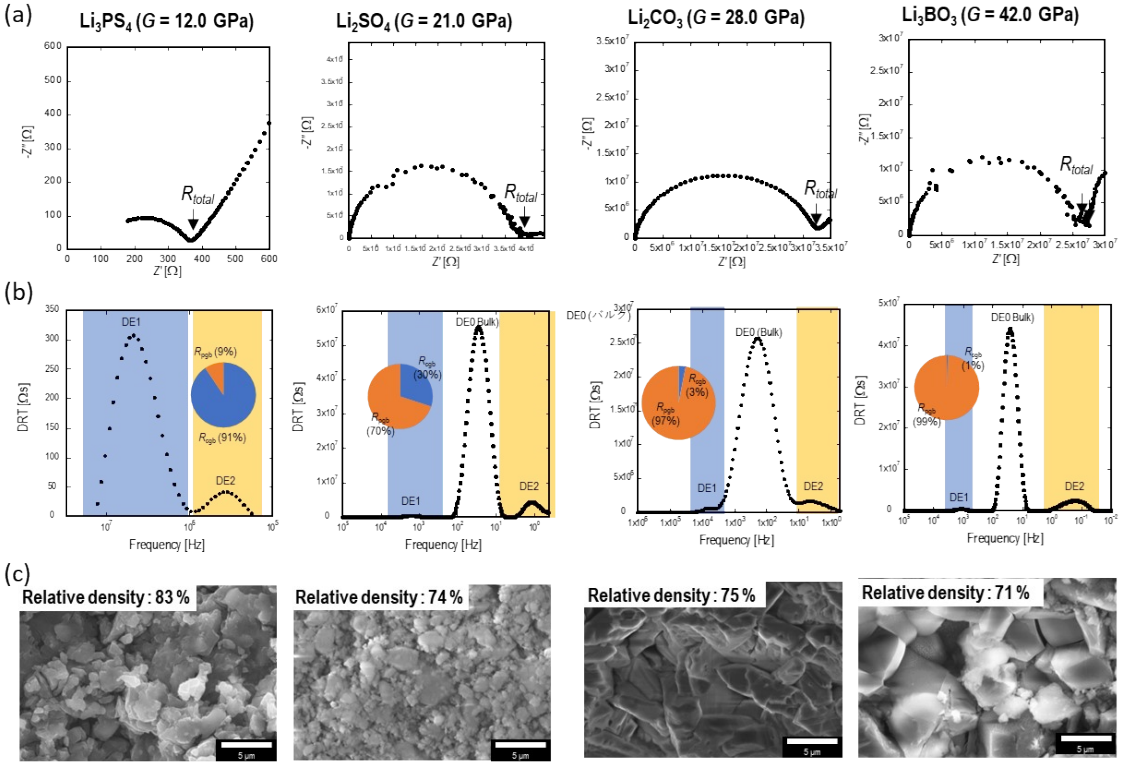

Fig. S5. Characterisation of pellets of the sulfide Li_3PS_4 and oxides Li_2SO_4, Li_2CO_3, and Li_3BO_3. (a) AC impedance results (Nyquist plots). Measurements for Li_2SO_4 and Li_3BO_3 were performed at an elevated temperature (100 °C) owing to their high resistivity. (b) DRT spectra. The pie chart shows the ratio of crystallite grain boundary resistance R_{cgb} and particle grain boundary resistance R_{pgb}. (c) Cross-sectional SEM images of the pellets; the relative densities are indicated.

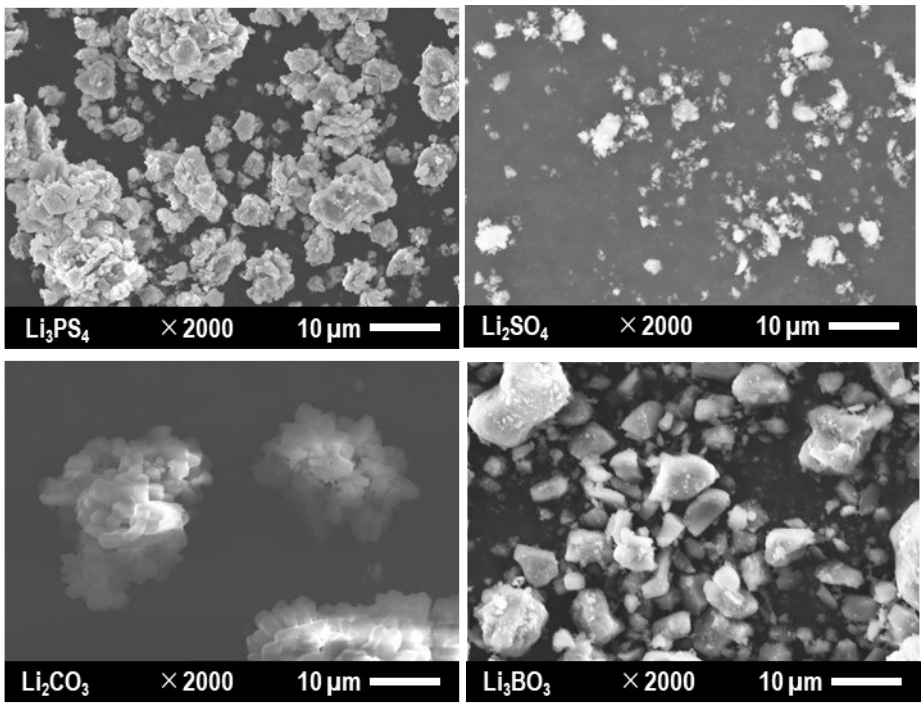

Fig. S6. Cross-sectional SEM images of the sulfide Li_3PS_4 and oxide Li_2SO_4, Li_2CO_3, and Li_3BO_3 powders.

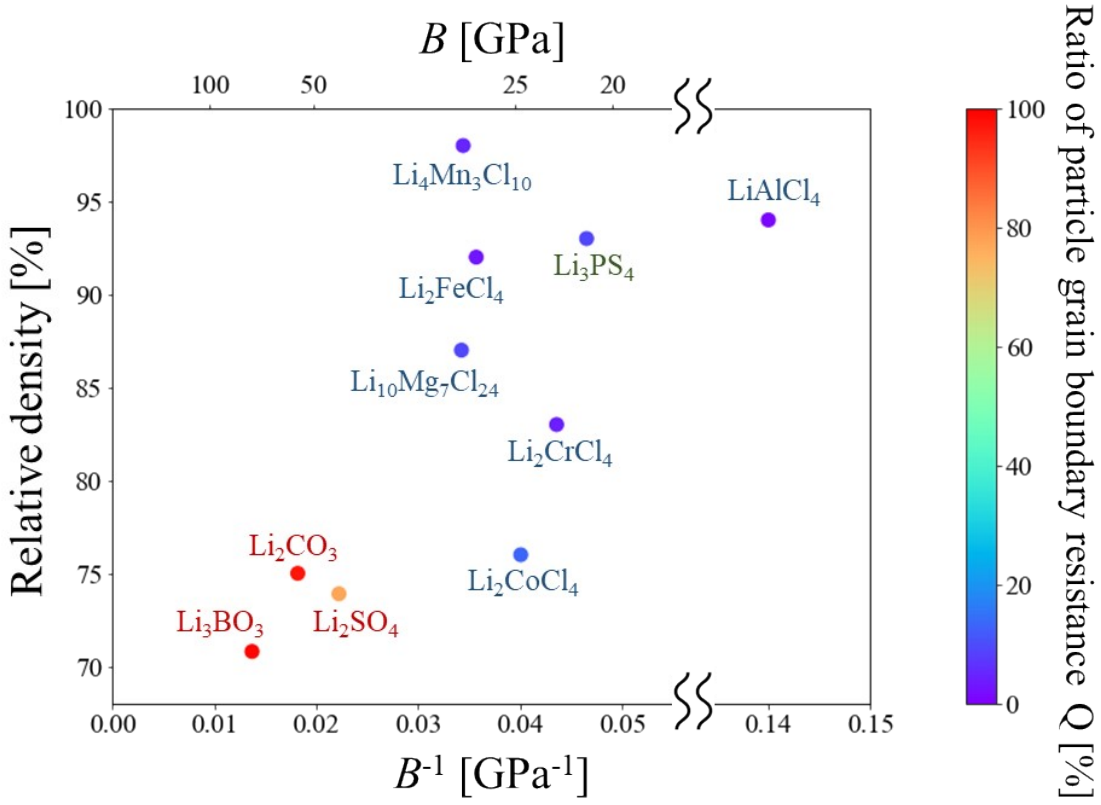

Fig. S7. Relationship among volumetric modulus *B*, relative density of the pellets, and ratio of particle grain boundary resistance to the total grain boundary resistance, *Q*, for the nine materials, including the six chlorides that were the focus of this study, that is, Li_2CoCl_4, Li_2CrCl_4, $Li_{10}Mg_7Cl_{24}$, $Li_4Mn_3Cl_{10}$, Li_2FeCl_4, and $LiAlCl_4$, as well as the oxides Li_2SO_4, Li_2CO_3, and Li_3BO_3 and the sulfide Li_3PS_4.

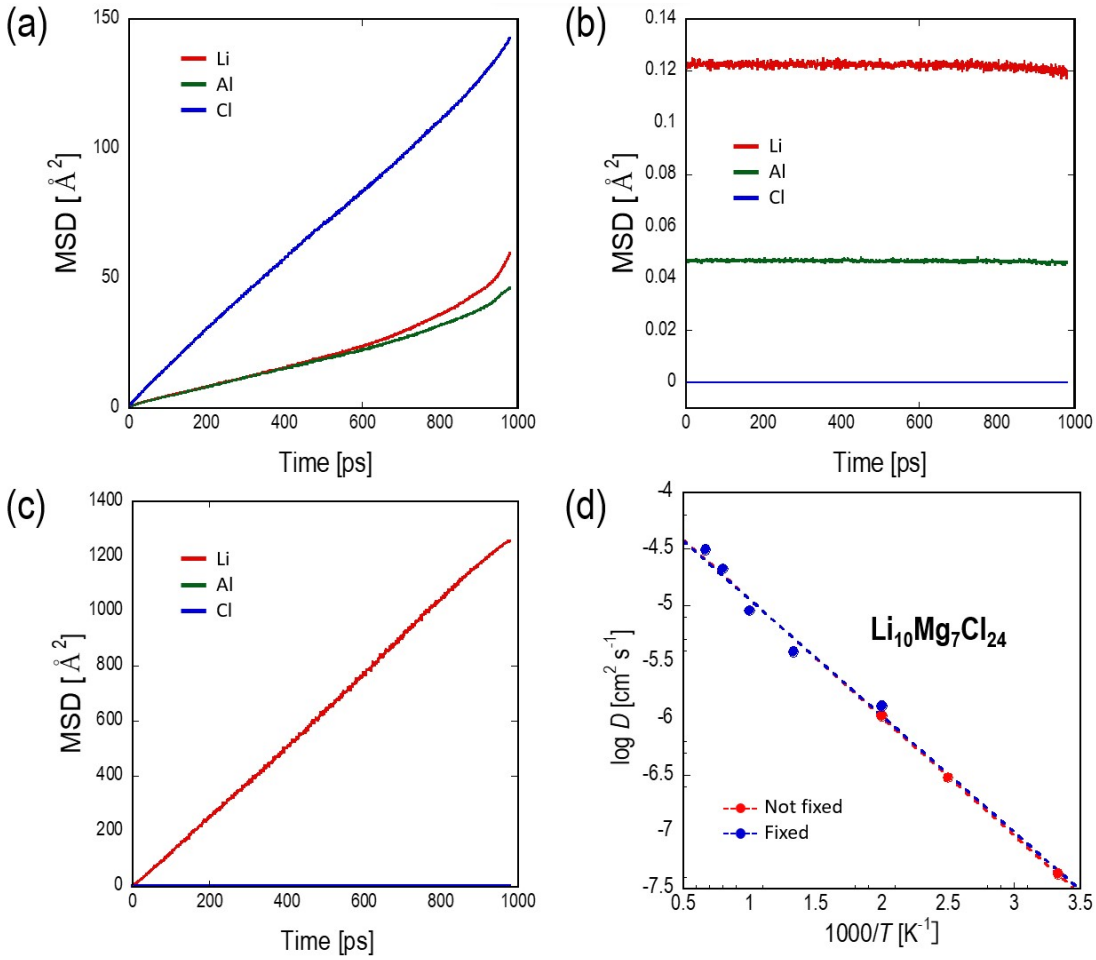

Fig. S8. Mean square displacement (MSD) plots from a representative Li-chloride molecular dynamics calculation ($LiAlCl_4$, mp-22983) performed using a high-throughput force field.[9] (a) MSD plot at 500 K obtained without fixing the anion positions. (b) MSD plots at 500 K obtained with the anion positions fixed. (c) MSD plot at 1000 K obtained with the anion positions fixed. (d) Arrhenius plots of diffusion coefficients obtained via molecular dynamics calculations using a high-throughput force field for a representative example of an LiCl material ($Li_{10}Mg_7Cl_{24}$, mp-530738). Red data points indicate the results of calculations at 300, 400, and 500 K obtained without fixing the anion positions. The blue data points show the results of calculations performed at 500, 750, 1000, 1250, and 1500 K obtained with the anion positions fixed.

Supplementary note: Li diffusivity evaluation via molecular dynamics (MD) simulations

In this study, molecular dynamics (MD) simulations were performed with the skeletal structure fixed, that is, the coordinates of the chlorides were fixed. This was because the melting points of chloride materials are low; therefore, the skeletal structure may collapse at the high temperatures commonly utilised in MD calculations. For example, Fig. S8 shows the results of MD simulations for $LiAlCl_4$. The melting point of $LiAlCl_4$ is 433 K. As can be observed in the mean square displacement (MSD) plot, $LiAlCl_4$ melts at 500 K with chlorine diffusion (Fig. S8(a)). Moreover, the frequency of Li diffusion events may not be sufficient to obtain statistics for calculating the Li diffusion coefficient at temperatures below 430 K. Therefore, the anion structure was fixed, and the Li diffusion coefficient was calculated via MD simulations at high temperatures. Fig. S8(c) shows the MSD plot from the MD calculation at 1000 K. Although no diffusion was observed for any element at 500 K (Fig. S8(b)), Li alone was observed to diffuse at 1000 K. The Li ion conductivity at 298 K calculated from the extrapolation of the Arrhenius plot in the high-temperature region with the ion positions fixed was 5.9×10^{-7} S cm^{-1}, which is close to the experimental value (1×10^{-6} S cm^{-1}). Furthermore, in the Arrhenius plot of the $Li_{10}Mg_7Cl_{24}$ (mp-530738) diffusion coefficient (Fig. S6(d)), the straight line for the data obtained with the anion positions fixed is almost identical to that for the data obtained without fixing the anion positions. This indicates that fixing the anion positions does not significantly affect the diffusion coefficient. Therefore, in this study, the MD simulations were performed at five temperatures (500, 750, 1000, 1250, and 1500 K) with the chloride ion positions fixed. The Li diffusion coefficients were calculated from the MSD slopes of other samples. Samples with an MSD slope of

almost zero, even at 1500 K, were considered to have zero ionic conductivity.

Table S1. Calculated values of Li diffusion coefficient $D_{\mathrm{Li},RT}$, energy above hull E_{Hull}, and shear modulus G for each of the Li–Cl compounds.

Material id	Chemical formula	$D_{\mathrm{Li},RT}$ [cm² s⁻¹]	E_{Hull} [eV atom⁻¹]	G [GPa]
mp-998591	$LiSnCl_3$	1.55×10^{-36}	0.008448336	5.461882569
mp-998230	$LiSnCl_3$	1.12×10^{-17}	0.018967877	6.755421796
mp-989583	$Rb_2LiInCl_6$	4.08×10^{-11}	0	12.00356415
mp-989579	$Rb_2LiTlCl_6$	9.14×10^{-13}	0.015591515	12.70132622
mp-989512	$LiTl_2InCl_6$	2.47×10^{-10}	0	14.51342755
mp-686087	$Li_3(Nb_2Cl_5)_8$	3.09×10^{-11}	0.012968019	-
mp-686004	$Li3ScCl_6$	1.16×10^{-17}	0.012203	12.72936733
mp-685992	Li_2CrCl_4	5.65×10^{-9}	0.073214274	12.92982901
mp-680167	$LiMo_6Cl_{13}$	1.25×10^{-7}	0.01127676	2.976522323
mp-677135	Li_2CoCl_4	0	1.648672956	20.28624775
mp-676752	Li_2FeCl_4	5.11×10^{-9}	0.202861054	6.430357728
mp-676683	**Li_2FeCl_4**	**8.77×10^{-9}**	0.031559694	10.68975814
mp-676361	$Li3ErCl_6$	3.50×10^{-17}	0	14.43590228
mp-676210	$LiTiCl_3$	6.89×10^{-11}	0.095064055	-20.4548349
mp-676109	Li_3InCl_6	5.31×10^{-23}	0	12.51176384
mp-675460	$LiTiCl_3$	1.87×10^{-7}	0.27596539	17.30447897
mp-606711	$Cs3LiCl_4$	8.73×10^{-7}	0.059343854	8.416746373
mp-571666	$CsLi_3Cl_4$	2.58×10^{-21}	0.028389297	10.7010079
mp-571612	LiW_6CCl_{18}	0	0.012219054	-
mp-571527	$Cs_2LiInCl_6$	2.62×10^{-9}	0	10.28838333
mp-571390	Cs_2LiCl_3	3.63×10^{-21}	0.024857768	9.841205638
mp-570869	$LiNb_3InCl_9$	2.48×10^{-18}	0.002247427	10.41429913
mp-570512	$LiWCl_6$	7.54×10^{-14}	0.012143757	-
mp-569117	$CsLi_2Cl_3$	4.60×10^{-9}	0.019124206	9.933433151
mp-567652	Cs_2LiYCl_6	4.67×10^{-6}	0	12.45602124
mp-567474	**Li_2CrCl_4**	**6.57×10^{-9}**	0.049856652	13.63073846
mp-532443	$Li_5V_5Cl_{16}$	2.49×10^{-8}	0.180230588	11.18693553
mp-531376	**$Li_4Mn_3Cl_{10}$**	**5.45×10^{-8}**	0.00403793	11.77195623
mp-530738	**$Li_{10}Mg_7Cl_{24}$**	**4.35×10^{-8}**	0.020200601	12.71821553
mp-505391	Li_6CoCl_8	1.05×10^{-31}	0.030864541	19.90232217

mp-38684	Li_2MgCl_4	4.10×10^{-11}	0.006588491	12.76243794
mp-38008	Li_2CdCl_4	8.22×10^{-6}	0.010504225	11.08787898
mp-36330	Li_2VCl_4	2.03×10^{-10}	0.011353206	12.39279916
mp-34457	Li_2CoCl_4	6.91×10^{-11}	0.141976284	18.731053
mp-34148	Li_2MnCl_4	8.66×10^{-15}	0.006057414	11.91999236
mp-29985	$LiNb_6Cl_{19}$	1.96×10^{-17}	0	5.889648047
mp-29582	Li_2CrCl_4	1.91×10^{-10}	0.046454547	10.3183314
mp-29344	$LiGaCl_3$	5.83×10^{-18}	0	10.35414277
mp-29250	Li_6VCl_8	0	0.012617101	19.91762251
mp-28828	Li_6FeCl_8	2.60×10^{-14}	0.092345903	19.03395232
mp-28463	$LiNb_3Cl_8$	1.72×10^{-9}	0	12.25143066
mp-28341	$LiGaCl_4$	9.24×10^{-10}	0	4.231483787
mp-28243	$RbLiCl_2$	2.30×10^{-18}	0.002885881	9.422648507
mp-28122	$LiGdCl_4$	0	0.00259213	10.43546087
mp-28068	$LiDy_2Cl_5$	1.96×10^{-19}	0.190573681	15.61583524
mp-23416	Li_2ZnCl_4	4.41×10^{-15}	0.012703998	12.51940231
mp-23364	$CsLiCl_2$	6.16×10^{-7}	0.012217325	8.678754387
mp-23361	Li_5CrCl_8	1.45×10^{-8}	0.011215566	15.582161
mp-22983	**$LiAlCl_4$**	**1.54×10^{-11}**	0	4.947485309
mp-22980	**Li_2CoCl_4**	**5.72×10^{-12}**	0.017858303	17.37988247
mp-22961	Li_2ZnCl_4	0	0.017143571	16.64195843
mp-1222796	Li_2CoCl_4	4.74×10^{-10}	0.156567239	20.73531746
mp-1222745	Li_2FeCl_4	0	0.1518639	12.77729035
mp-1211124	Li_6NiCl_8	6.22×10^{-17}	0	20.11273463
mp-1210931	$LiFeCl_4$	1.39×10^{-9}	0	5.778377258
mp-1210835	Li_2BeCl_4	6.47×10^{-15}	0.00851579	14.83897918
mp-1206553	$Rb_2LiRuCl_6$	9.83×10^{-11}	0	3.510010077
mp-1206403	Rb_2LiVCl_6	9.50×10^{-23}	0.02154604	14.31397569
mp-1206399	Rb_2LiVCl_6	5.89×10^{-11}	0	-0.906828953
mp-1206187	$Rb_2LiRhCl_6$	1.47×10^{-10}	0	5.051879921
mp-1205883	$Rb_2LiHoCl_6$	3.02×10^{-9}	0.002265448	12.70792524
mp-1205649	$LiSc(TlCl_3)_2$	0	0	14.72005544
mp-1198972	$Li_6Zr_6HCl_{18}$	7.60×10^{-31}	0.020682633	16.04785159
mp-1190687	$CsLi_2Cl_3$	6.56×10^{-22}	0.001272549	7.136903266

mp-1189625	$Cs_2LiScCl_6$	4.85×10^{-8}	0	11.30032817
mp-1188344	$CsLiCl_2$	1.36×10^{-8}	0	7.253265462
mp-1120734	Cs_3LiCl_4	6.76×10^{-13}	0.214779303	6.123746748
mp-1114583	Rb_2LiYCl_6	0	0.00494897	12.22078602
mp-1114579	$Rb_2LiTaCl_6$	2.24×10^{-14}	0.112382972	14.53427949
mp-1114571	$Rb_2LiNdCl_6$	1.65×10^{-16}	0.032174464	11.06247265
mp-1114567	$Rb_2LiLaCl_6$	3.02×10^{-9}	0.042283446	9.016485169
mp-1114566	$Rb_2LiErCl_6$	4.43×10^{-23}	0.000185609	13.06959628
mp-1114565	$Rb_2LiDyCl_6$	1.06×10^{-8}	0.003880535	12.595736
mp-1114562	$Rb_2LiBiCl_6$	5.54×10^{-8}	0	11.24792255
mp-1114431	$Rb_2LiTbCl_6$	2.60×10^{-13}	0.005710754	12.42760706
mp-1114429	$Rb_2LiScCl_6$	1.48×10^{-9}	0	13.92881696
mp-1114428	$Rb_2LiSbCl_6$	8.99×10^{-24}	0	11.77810497
mp-1114423	$Rb_2LiMoCl_6$	2.08×10^{-21}	0	13.60593862
mp-1114421	$Rb_2LiLuCl_6$	2.93×10^{-16}	0	16.93907393
mp-1114417	$Rb_2LiCeCl_6$	0	0.084097757	9.833513203
mp-1114414	$Rb_2LiAuCl_6$	0	0.124259526	7.598634616
mp-1114176	$K_2LiTaCl_6$	9.53×10^{-8}	0.144685504	13.74853025
mp-1113945	$Na_2LiAuCl_6$	4.21×10^{-14}	0.233189439	3.954990039
mp-1113921	$Na_2LiErCl_6$	8.49×10^{-29}	0.118538205	12.25557094
mp-1113912	$Na_2LiInCl_6$	2.52×10^{-12}	0.131522275	11.56953232
mp-1113903	$Na_2LiScCl_6$	0	0.103259453	13.46057812
mp-1113898	$Na_2LiTlCl_6$	2.21×10^{-15}	0.137094961	11.27047756
mp-1113840	$Na_2LiLaCl_6$	2.32×10^{-9}	0.176806233	9.645898997
mp-1113839	$Na_2LiDyCl_6$	5.75×10^{-18}	0.11895373	11.77114339
mp-1113837	$Na_2LiBiCl_6$	7.14×10^{-33}	0.121728747	10.16847696
mp-1113742	Na_2LiYCl_6	0	0.125927748	12.22403797
mp-1113318	$Na_2LiTbCl_6$	2.24×10^{-10}	0.122539436	11.92362953
mp-1113317	$Na_2LiSbCl_6$	2.26×10^{-7}	0.145280272	9.91495411
mp-1113316	$Na_2LiLuCl_6$	1.05×10^{-15}	0.112977848	13.13890121
mp-1113026	$Cs_2LiAuCl_6$	0	0.126226952	9.229461978
mp-1113018	$Cs_2LiDyCl_6$	1.90×10^{-9}	0	12.5318003
mp-1113012	$Cs_2LiMoCl_6$	1.76×10^{-10}	0.031926	12.64319487
mp-1113004	$Cs_2LiScCl_6$	0	0.011216129	13.45870136

mp-1112999	$Cs_2LiTlCl_6$	9.73×10^{-11}	0.017419603	12.60102971
mp-1112669	$Cs_2LiTbCl_6$	3.25×10^{-11}	0	12.4310478
mp-1112613	$Cs_2LiErCl_6$	6.71×10^{-6}	0	12.78116225
mp-1111932	$K_2LiScCl_6$	4.51×10^{-14}	0	13.99036943
mp-1111678	$K_2LiAuCl_6$	0	0.140470215	6.06137832
mp-1111675	$K_2LiCeCl_6$	2.49×10^{-6}	0.056584505	56.37672967
mp-1111672	$K_2LiInCl_6$	1.42×10^{-12}	0.02724929	12.00041516
mp-1111666	$K_2LiMoCl_6$	3.86×10^{-11}	0.037788106	13.48223181
mp-1111664	$K_2LiSbCl_6$	1.02×10^{-19}	0.039358543	11.00633077
mp-1111660	$K_2LiTlCl_6$	2.01×10^{-18}	0.036989102	12.27761852
mp-1111654	K_2LiYCl_6	2.89×10^{-5}	0.026140421	11.7428968
mp-1111288	Li_3InCl_6	1.86×10^{-9}	0.266298984	11.24132776
mp-1111284	Li_3ScCl_6	0	0.244241486	13.03989689
mp-1111273	$K_2LiEuCl_6$	2.68×10^{-25}	0.042051628	4.393139049
mp-1111262	$Li_2ScCuCl_6$	1.20×10^{-14}	0.273103071	10.03021651
mp-1111261	$K_2LiBiCl_6$	0	0	6.57466444
mp-1111259	$K_2LiDyCl_6$	1.75×10^{-9}	0.025984887	12.1829594
mp-1111257	$K_2LiLaCl_6$	2.36×10^{-21}	0.071879093	10.23133184
mp-1111256	$K_2LiErCl_6$	1.97×10^{-18}	0.020649807	12.82853398
mp-1111149	Li_3SbCl_6	1.34×10^{-10}	0.293585337	10.37733826
mp-1111130	$K_2LiTbCl_6$	1.82×10^{-7}	0.032657765	11.8677904
mp-1111126	$K_2LiLuCl_6$	3.26×10^{-11}	0	12.40319891
mp-1111123	$Li_2InCuCl_6$	1.08×10^{-8}	0.259715712	9.716304577
mp-1111120	$Li_2CuSbCl_6$	3.09×10^{-11}	0.288497732	9.226022992

Table S2. Conductivity diffusion coefficients obtained from AC impedance measurements for six chlorides (Li_2CoCl_4, Li_2CrCl_4, $Li_{10}Mg_7Cl_{24}$, $Li_4Mn_3Cl_{10}$, Li_2FeCl_4, and $LiAlCl_4$).

Chemical formula	$D_{Li,\,RT}$ [$cm^2\,s^{-1}$]
$Li_{10}Mg_7Cl_{24}$	4.8×10^{-11}
$LiAlCl_4$	2.8×10^{-10}
Li_2CrCl_4	2.3×10^{-12}
$Li_4Mn_3Cl_{10}$	2.6×10^{-10}
Li_2FeCl_4	2.8×10^{-10}
Li_2CoCl_4	3.8×10^{-11}

Table S3. Resistance decomposition results for the chlorides Li_2CoCl_4, Li_2CrCl_4, $Li_{10}Mg_7Cl_{24}$, $Li_4Mn_3Cl_{10}$, Li_2FeCl_4, and $LiAlCl_4$. DE-*R*, DT-*T*, and DE-*C* indicate the resistance, relaxation time, and capacitance, respectively, obtained from DRT analysis. *d*, C_{cb}, and *Q* indicate the crystallite size calculated using the Halder–Wagner method, capacitance of the crystallite grain boundary estimated using the Brickwork model, and resistance ratio of the particle grain boundary.

Compound	DE1-*R* / Ω	DE1-*T* / s	DE1-*C* / F	DE2-*R* / Ω	DE2-*T* / s	DE2-*C* / F	*d* / Å	C_{cb} / F	*Q* / %
Li_2CoCl_4	2.6×10^4	3.6×10^{-6}	1.4×10^{-10}	4.2×10^3	3.6×10^{-4}	8.5×10^{-8}	111	1.1×10^{-10}	13
Li_2CrCl_4	2.2×10^5	2.9×10^{-5}	1.3×10^{-10}	9.7×10^3	4.0×10^{-3}	4.1×10^{-7}	290	2.9×10^{-10}	4
$Li_{10}Mg_7Cl_{24}$	6.9×10^4	8.8×10^{-6}	1.3×10^{-10}	6.8×10^3	1.8×10^{-3}	2.6×10^{-7}	115	1.2×10^{-10}	9
$Li_4Mn_3Cl_{10}$	3.2×10^3	9.6×10^{-7}	3.0×10^{-10}	1.9×10^2	5.8×10^{-5}	3.1×10^{-7}	152	1.5×10^{-10}	4

Table S4. Resistance decomposition results for the sulfide Li_3PS_4 and oxides Li_2SO_4, Li_2CO_3, and Li_3BO_3. DE-*R*, DT-*T*, and DE-*C* indicate the resistance, relaxation time, and capacitance, respectively, obtained from DRT analysis. *d*, C_{cb}, and *Q* indicate the crystallite size calculated using the Halder–Wagner method, capacitance of the crystallite grain boundary estimated using the Brickwork model, and resistance ratio of the particle grain boundary.

Compound	DE1-*R* / Ω	DE1-*T* / s	DE1-*C* / F	DE2-*R* / Ω	DE2-*T* / s	DE2-*C* / F	*d* / Å	C_{cb} / F	*Q* / %
Li_3PS_4	2.6×10^2	2.4×10^{-8}	9.2×10^{-11}	27	5.7×10^{-7}	2.1×10^{-8}	98	9.8×10^{-11}	9
Li_2SO_4	8.4×10^5	1.3×10^{-3}	1.6×10^{-9}	2.8×10^6	9.7×10^{-2}	3.6×10^{-8}	320	3.2×10^{-10}	77
Li_2CO_3	1.3×10^4	2.5×10^{-6}	2.0×10^{-10}	7.2×10^5	2.2×10^{-2}	3.1×10^{-8}	355	3.6×10^{-10}	97
Li_3BO_3	2.6×10^4	1.0×10^{-5}	3.9×10^{-10}	4.2×10^6	2.4×10^{-2}	5.7×10^{-9}	325	3.3×10^{-10}	99

References

1 N. Tanibata, S. Takimoto, K. Nakano, H. Takeda, M. Nakayama and H. Sumi, *ACS Mater Lett*, 2020, **2**, 880–886.

2 S. Aizu, S. Takimoto, N. Tanibata, H. Takeda, M. Nakayama and R. Kobayashi, *Journal of the American Ceramic Society*, 2023, **106**, 3035–3044.

3 N. Tanibata, M. Kato, S. Takimoto, H. Takeda, M. Nakayama and H. Sumi, *Advanced Energy and Sustainability Research*, 2020, **1**, 2000025.

4 H. Xia, L. Lu and G. Ceder, *J Power Sources*, 2006, **159**, 1422–1427.

5 K. Tang, X. Yu, J. Sun, H. Li and X. Huang, *Electrochim Acta*, 2011, **56**, 4869–4875.

6 N. Kuwata, M. Nakane, T. Miyazaki, K. Mitsuishi and J. Kawamura, *Solid State Ion*, 2018, **320**, 266–271.

7 F. N. Sayed, M. B. Sreedhara, A. Soni, U. Bhat, R. Datta, A. J. Bhattacharyya and C. N. R. Rao, *Mater Res Express*, , DOI:10.1088/2053-1591/ab3e19.

8 N. Imanishi, K. Kanamura and Z. I. Takehara, *J Electrochem Soc*, 1992, **139**, 2082–2087.

9 R. Kobayashi, *J Open Source Softw*, 2021, **6**, 2768.